

# An Experimental Comparison of a Hierarchical Range Image Segmentation Algorithm

Gustavo Osorio

National University of Colombia

Pierre Boulanger

University of Alberta

Flavio Prieto

National University of Colombia

**Abstract** This paper describe a new algorithm to segment range images into continuous regions represented by Bézier polynomials. The main problem in many segmentation algorithms is that it is hard to accurately detect at the same time large continuous regions and their boundary location. In this paper, a Bayesian framework is used to determine through a region growing process large continuous regions. Following this process, an exact description of the boundary of each region is computed from the mutual intersection of the extracted parametric polynomials followed by a closure and approximation of this new boundary using a gradient vector flow algorithm. This algorithm is capable of segmenting not only polyhedral objects but also sculptured surfaces by creating a network of closed trimmed Bézier surfaces that are compatible with most CAD systems. Experimental results show that significant improvement of region boundary localization and closure can be achieved. In this paper, a systematic comparison of our algorithm to the most well known algorithms in the literature is presented to highlight its performance.

**Keywords:** Range Image, Segmentation, Gradient Flow, Bayesian Methods

## 1 Introduction

The scientific literature reports many segmentation algorithms. As classified by Hoover et al. [3] algorithms for range image segmentation falls into two basic categories, i.e., 1) region-based or 2) edge-based. There are also the so called hybrid techniques that use both region and edge information to guide the segmentation process. In many ways the proposed segmentation algorithm fall into this category. In Hoover et al. ground braking work, four of the state-of-the-art range image segmentation algorithms were analyzed systematically relative to a

ground truth segmented by an expert. One of the major conclusion of this analysis is that range image segmentation is still not really a solved problem even for simple scenes containing only polyhedral objects. Later Jiang et al. [6] and Min et al. [10] confirmed those results by further refining this comparison technique. The main problem is that in most algorithms, it is hard to accurately detect at the same time geometric surfaces and exact edge locations between those surfaces. Hoover et al. segmentation comparison framework is widely used for evaluating segmentation algorithms, including segmentation algorithms [11] for curved surface and in [10] to compute optimal segmentation parameters. The main purpose of this paper is to present briefly our segmentation algorithm and to compare its performance to the best algorithms in the literature using Hoover's methodology.

In this paper, we will first give a brief description of our segmentation algorithm followed by a description on how to improve boundary localization and closure using parametric re-intersection and a gradient vector flow algorithm. Then a brief description of Hoover's comparison methodology is presented. In the experimental result section, our algorithm is compared to the most efficient segmentation algorithms in the literature. We will demonstrate how the segmentation accuracy is significantly improved by surface re-intersection and how it compares to the best segmentation algorithm for planar regions. Finally, more segmentation results are presented followed by a short discussion on the comparison methodology.

## 2 Hierarchical Segmentation

The Hierarchical Segmentation algorithm used in this work is based on the optimal clustering of first order seed regions into larger regions based on a

Bayesian similarity measurement. This algorithm was presented in [1] in the context of segmenting simultaneously range and color images, because most algorithms we are planning to compare with only work on range signals it was decided to ignore the intensity signal for the moment. The main idea behind our algorithm is to represent a range image with a simple model, and then produce modifications to the model using more complex geometric primitives based on a statistical inference process. Lets review briefly the basic steps of our algorithm:

- **Initial partition.** The objective of this processing stage is to produce an optimal set of seed regions represented by first order Bézier polynomials that do not include depth and orientation discontinuities. To compute the parameters of each seed region an algorithm based on a robust fitting technique is used to avoid contamination by undetected discontinuities in a neighborhood. The result is an adjacency graph of first order regions or points represented by the coefficients of the Bézier polynomial.
- **Clustering.** A region to region and region to point clustering algorithm is used to produce larger regions of first order surfaces. In this algorithm the grouping process is determined by computing a similarity function based on a Bayesian analysis between adjacent surfaces and points. The tracking and the management of the optimal grouping is performed using a hierarchical data structure. Optimal grouping of surfaces is performed until a predetermined approximation threshold is reached.
- **Generalization.** Following this process, some surfaces can be generalized with a more complex model (i.e. second order Bézier). The decision to change to a higher order surface is determined by an optimal statistical analysis that use F-distribution to determine if the higher order model is statistically justified. Following this generalization process the clustering process is repeated until the approximation threshold is reached again.

Figure 1 shows the segmentation results using our algorithm for images with first and second order surfaces on an image from the University of South Florida [12] range image database.

Following a comparison analysis between our algorithm and the best one in the literature proposed by the University of Bern [8], it is clear the our algorithm had some problems for planar surfaces. One of the main source of error is *Over-Segmentation*. This

problem can easily be resolved by merging surfaces where the difference between the normal vectors is not grater than 10 degrees. In Figure 2, one can see the result of this merging process.

Furthermore, a second source of error in our segmentation process is associated with the precision of the region boundaries. One can see in Figure 3 a comparison of the regions boundaries produced by the University of Bern algorithm and ours. There is obviously a problem that is due to noise and the fact that we are not really using planar models but first order Bézier functions.

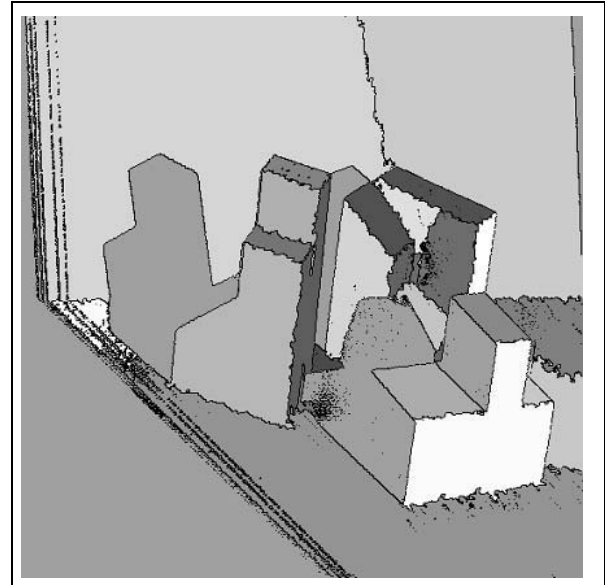


Figure 1: Hierarchical segmentation results for one of the USF range image.

### 3 A Posteriori Computation of Region Contours Using Exact Surface Re-Intersection

Edge detection technics are widely used in order to obtain the contour of objects. In reflectance images there contours are mainly due to abrupt changes in the reflective properties of an object or by shadows. In range images there are different kinds of discontinuities that can be classified as depth and orientation. Some authors include a third kind called smooth discontinuity ("crease edges") which refers to continuous changes in the normal vector but with abrupt changes in the curvature. There are basically two ways to solve the problem of edge localization

namely using local geometrical properties or using global information. In this paper, we present a new technique to compute those region boundaries by performing a re-intersection between adjacent surfaces followed by a the closure and approximation of those contours using a gradient flow algorithm.

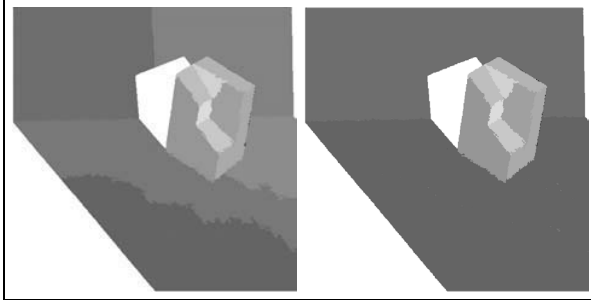


Figure 2: Solution to over-segmentation using a normal threshold: (Left) *Over-Segmented* result, (Right) Segmentation result after merging with a threshold of 10 degrees.

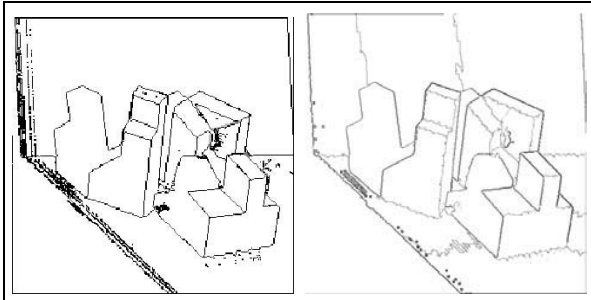


Figure 3: (Left) Segmented results using University of Bern algorithm, (Right) Segmented results using our algorithm.

### 3.1 Parametric Surface Re-

In order to achieve a better performance and to improve the localization of region boundaries the following algorithm is proposed. The main idea is to include the global information obtained in the previous segmentation stage and to recompute the boundaries intersection by using the parametric equations of the adjacent regions expressed by Equation 1. Equation 2 shows the transformation matrix ( $\mathbf{A}$ ) for a first order parametric polynomial.

$$\begin{bmatrix} a_{11} & a_{12} & a_{13} \\ a_{21} & a_{22} & a_{23} \\ a_{31} & a_{32} & a_{33} \end{bmatrix} \begin{bmatrix} 1 \\ u \\ v \end{bmatrix} + \begin{bmatrix} C_x \\ C_y \\ C_z \end{bmatrix} = \begin{bmatrix} x \\ y \\ z \end{bmatrix} \quad (1)$$

$$\mathbf{A}_i \cdot \mathbf{P} = \mathbf{S}_i \quad (2)$$

where

$$\mathbf{A} = \begin{bmatrix} a_{11} + C_x & a_{12} & a_{13} \\ a_{21} + C_y & a_{22} & a_{23} \\ a_{31} + C_z & a_{32} & a_{33} \end{bmatrix}; \mathbf{P} = \begin{bmatrix} 1 \\ u \\ v \end{bmatrix}; \mathbf{S} = \begin{bmatrix} x \\ y \\ z \end{bmatrix}. \quad (3)$$

For every surface  $\mathbf{S}_i$  the transformation matrix  $\mathbf{A}_i$  is obtained. From Equation 2, it is possible to obtain the equation for the planar surface  $\mathbf{S}_i$  as follow:

Let  $\mathbf{O}_i$  be a point belonging to the plane, which is known after the segmentation process (see Equation 4). Let  $\mathbf{A}_i$  be the transformation matrix from the parametric space  $(u, v)$  to the 3-D space  $(x, y, z)$ , where the normal vector  $\mathbf{n}_i$  to the plane  $\mathbf{S}_i$  in the space  $(x, y, z)$  is given by Equation 5, and the expression for the plane given by Equation 6.

$$\mathbf{O}_i = \begin{bmatrix} C_{x_i} \\ C_{y_i} \\ C_{z_i} \end{bmatrix} \in \mathbf{S}_i \quad (4)$$

$$\mathbf{n}_i = \frac{\frac{\partial \mathbf{S}_i}{\partial u} \times \frac{\partial \mathbf{S}_i}{\partial v}}{\left\| \frac{\partial \mathbf{S}_i}{\partial u} \times \frac{\partial \mathbf{S}_i}{\partial v} \right\|} \quad (5)$$

$$(\mathbf{O}_i + \mathbf{V}) \cdot \mathbf{n}_i = 0 \quad (6)$$

Once the parameters for every surface in the image has been determined, is possible to find the parametric function of the straight line produced by the intersection of adjacent planes as follow:

Let  $\mathbf{p}_{ij}$  a point in both regions  $\mathbf{S}_i$  and  $\mathbf{S}_j$ , and let  $\mathbf{V}_{ij}$  be a vector parallel to the straight line generated by the intersection of the planes, and given by Equation 7, then the parametric representation of the intersection is given by Equation 8.

$$\mathbf{V}_{ij} = \mathbf{n}_i \times \mathbf{n}_j \quad (7)$$

$$t \cdot \mathbf{V}_{ij} + \mathbf{p}_{ij} = \mathbf{V} \quad (8)$$

Figure 4(left) illustrates all the intersection lines for one plane and in Figure 4(right) the projection of all border points into these lines. Figure 5 shows the same result for an image with one object.

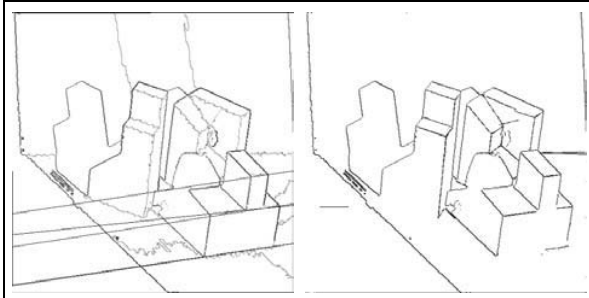


Figure 4: Original and improved boundaries using the parametric re-intersection of the the surface regions.

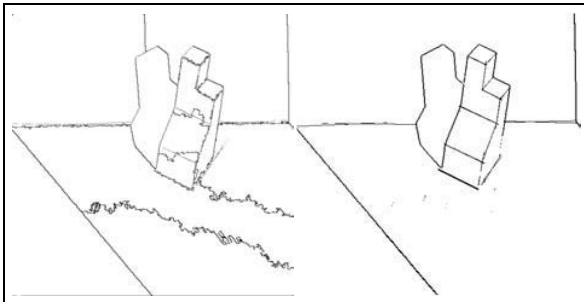


Figure 5: Results using the parametric re-intersection for an image with one object.

### 3.2 Closing and Approximating Contours with Gradient Vector Flow Algorithm

After defining the analytical expression for the segments that form the border of every single surface in the image, it is essential to obtain a reduce and closed contour. This is a necessary condition in order to be compatible with CAD systems. Several approaches can be used to solve this problem. For this paper an active contour algorithms developed for intensity images was adapted for this purpose. In 1987, Kass *et al.* [9] have introduce an active contours method, where the minimization of the sum of a series of energy terms leads to a smooth and close contour. In contrast with the traditional algorithms for border detection, this is a variational method based on solving partial differential equation representing a compromise between smoothness and localization. This algorithm presents several advantages which are interesting for our purposes since it can produce a close contour using a parametric representation. On the other hand one of the main drawback of this algorithm is that it is strongly dependant on initial conditions.

An active contour is a continuous parametric curve under the influence of internal and external forces. The internal forces are related to the first and second derivatives of the curve. The external force usually are defined as a force field that leads the curve towards the final contour, and is directly dependant on the image. One of the widely used algorithms for the computation of the external force is to obtain a force field based on the gradient of an image. This approach has leads to the formulation of the Gradient Vector Flow (GVF) [13] algorithm and the Generalized Gradient Vector Flow (GGVF) [14] algorithm that provide a significant improvement in the convergence rate and its robustness to the initial estimate.

Figures 6 and 7 are representative of the process to obtain the parametric boundary using active contours with the GGVF algorithm. Figure 6(left) shows the initial contour that is the boundary for one region using the hierarchical segmentation algorithm. In 6(right) the new boundaries provided by the parametric re-intersection is used to generate a Generalized Gradient Vector Flow (GGVF) illustrated in Figure 7(left). Figure 7(right) shows the result obtained when the process is applied to all regions in the image.

Probably the most interesting contribution of this technique is the reduction of dimensionality in the representation of the boundary given that it is possible to describe with few points a whole boundary.

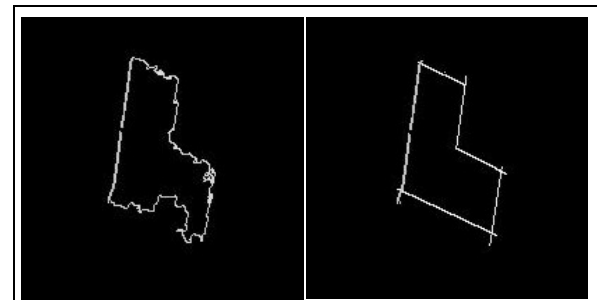


Figure 6: Initial contour (left). Re-intersected contour (right).

In the next section, we will analyze how our new modified algorithm compares to the best one in the literature.

## 4 Experimental Comparison Methodology

This section describe briefly the methodology used to compare the performance of various segmentation algorithms with ours. For a more detailed description see the work of A. Hoover *et al* [4].

### 4.1 Segmentation Definition

In the evaluation methodology proposed by A. Hoover *et al* [5], a formal definition of the segmentation process is used and our algorithm was mapped into this framework. This definitions has been proposed by some other authors as R. C. Gonzales [2] and is repeated here for completeness.

Let  $\mathbf{R}$  be a representation of the region of the complete image. *Segmentation* can be defined as the process of dividing  $\mathbf{R}$  in  $n$  subregions,  $\mathbf{R}_1, \mathbf{R}_2, \dots, \mathbf{R}_n$  in such a way that it satisfies:

1.  $\bigcup_{i=1}^n \mathbf{R}_i = \mathbf{R}$ ,
2.  $\mathbf{R}_i$  is a connected region for  $i=1,2,\dots,n$ ,
3.  $\mathbf{R}_i \cap \mathbf{R}_j = \emptyset$  for all  $i \neq j$ ,
4.  $P(\mathbf{R}_i) = \text{TRUE}$  for  $i=1,2,\dots,n$
5.  $P(\mathbf{R}_i \cup \mathbf{R}_j) = \text{FALSE}$  for  $i \neq j$ .

where  $P(\mathbf{R}_i)$  is a predicate for the elements belonging to  $\mathbf{R}_i$  and  $\emptyset$  is the empty set. In the particular case of range images, it is possible to have none valid elements produced by undesired phenomena inherent to the acquisition process such as shadows, corners or saturation noise.

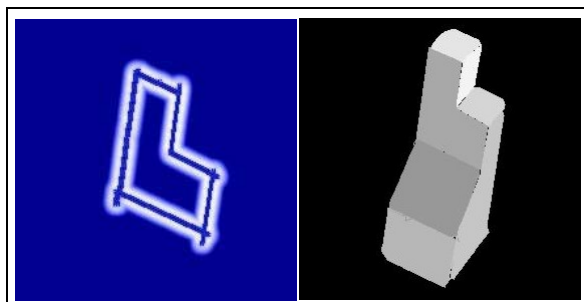


Figure 7: Generalized gradient vector flow field (left). Parametric boundaries for the hole image (right).

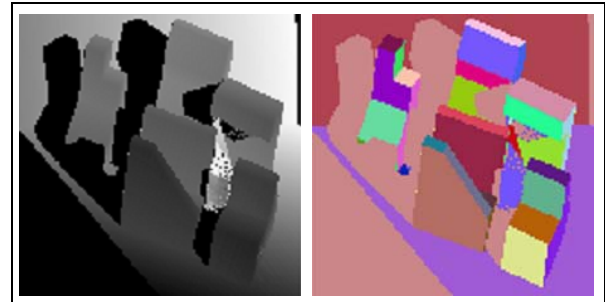


Figure 8: One of the USF range image used for the evaluation.

### 4.2 Test Images

For this work a database of 40 images, acquired with a structured light scanner producing range images of size  $512 \times 512$  with 8 bits per pixel was used. The database was made available for free by the University of South Florida [12]. The sensor also produce an associated intensity images of 8 bits per pixel which was not used because most other algorithms only process the range signal. Every image has different level of complexity according to the number of objects and surfaces to be segmented. All the objects in this database are polyhedral.

For the comparison process, every range image has a ground truth image associated created by hand segmentation performed by a human expert and the real angles of the normal vector for every surface is known. In Figure 8 an instance of the test images is shown.

### 4.3 Performance Measures

The comparison between the automatic segmentation (*Machine Segmentation, MS*) and the manual segmentation(*Ground Truth Segmentation, GT*) was performed as follows: Let  $M$  be the number of regions in the *MS* image, and  $N$  the number of regions in the *GT* image. Let  $P_m$  be the number of pixels in the *MS* region  $R_m$  (where  $m=1\dots M$ ). In the same way, let  $P_n$  be the number of pixels in the *GT* region  $R_n$  (where  $n=1\dots N$ ). Let  $O_{mn} = R_m \cap R_n$  be the number of pixels that simultaneously belongs to regions  $R_m$  and  $R_n$ . According to this definition in the case without overlapping between regions produces that  $O_{mn} = 0$ , and the case with a complete overlapping produces  $O_{mn} = P_m = P_n$ .

Then, it is possible to build the  $M \times N$  table, with the  $O_{mn}$  values, for  $m=1\dots M$  and  $n=1\dots N$ . This result will be used to calculate the overlapping index for every region in the *MS* image

as  $(O_{mn}/P_m$  and in the *GT* image as  $O_{mn}/P_n$ ). This indexes provide the discriminant information to classify every segmented region as one out of five classes: ***Correct Detection, Over-Segmentation, Under-Segmentation, Missed*** and ***Noise***. Over-Segmentation refers to a multiple detection of a single surface. Under-Segmentation refers to a merge of surfaces into a single one. A Missed occurs when the segmentation algorithm is not successful in the detection of a surface that appears in the image, and Noise occurs when the algorithm detects a surface that is not present in the image. The equations to classify every surface uses a threshold  $T$ , in the interval  $0.5 < T \leq 1.0$ . The value of  $T$  is determined by:

1. **Correct Detection.** Two regions,  $(R_m)$  in the *MS* image and  $R_n$  in the *GT* image are classified as a *Correct Detection* if:
  - (a)  $O_{mn} \geq T \times P_m$  (at least  $T$  percent of the pixels in  $R_m$  of the *MS* image, are marked as belonging to  $R_n$  in the *GT* image), **and**
  - (b)  $O_{mn} \geq T \times P_n$  (at least  $T$  percent of the pixels in  $R_n$  of the *GT* image, are marked as belonging to  $R_m$  in the *MS* image).
2. **Over-Segmentation.** One region  $R_n$  in the *GT* image, and a set of regions  $R_{m_1}, \dots, R_{m_x}$  in the *MS* image, where  $2 \leq x \leq M$ , are classified as an instance of *Over-Segmentation* if:
  - (a)  $\forall i \in x, O_{m_i n} \geq T \times P_m$  (for all  $i$ , at least  $T$  percent of the pixels in each region  $R_{m_i}$  of the *MS* image also belong to  $R_n$  in the *GT* image), **and**
  - (b)  $\sum_{i=1}^x O_{m_i n} \geq T \times P_n$  (at least  $T$  percent of the pixels of  $R_n$  in the *GT* image also belong to the union of the regions  $R_{m_1}, \dots, R_{m_x}$  in the *MS* image).
3. **Sub-Segmentation.** Given a set of regions  $R_{n_1}, \dots, R_{n_x}$ ,  $2 \leq x \leq M$ , in a *GT* image, then one region  $R_m$  in a *MS* image is classified as an instance of *Sub-Segmentation* if:
  - (a)  $\sum_{i=1}^x O_{m n_i} \geq T \times P_m$  (at least  $T$  percent of the pixels in  $R_m$  of the *MS* image, also belong to the union of regions  $R_{n_1}, \dots, R_{n_x}$  in the *GT* image), **and**
  - (b)  $\forall i \in x, O_{m n_i} \geq T \times P_m$  (at least  $T$  percent of the pixels in  $R_{n_i}$  of the *GT* image also belong to  $R_m$  in the *MS* image).

4. **Missed.** A region  $R_n$  of the *GT* image that is no classified as an instance of *Correct Detection, Over-Segmentation* or *Under-Segmentation* is classified as *Missed*.

5. **Noise.** A region  $R_m$  of the *MS* image that is no classified as an instance of *Correct Detection, Over-Segmentation* or *Under-Segmentation* is classified as *Noise*.

Even though these indexes produce a classification for every surface in the images *GT* and *MS*, this classification is not unique for  $T < 1.0$ . Furthermore, for the range  $0.5 < T < 1.0$ , every region can eventually contribute to three categories (*Correct Detection, Over-Segmentation* or *Under-Segmentation*). In the case more than one definition is satisfied, the region is classified according to the maximum index.

The "perfect" segmentation algorithm should be able to correctly detect all the regions with tolerance 1.0, and without instances of *Over-Segmentation, Under-Segmentation, Missed* or *Noise*.

## 5 Results

In the literature, one can find performance evaluation for seven segmentation techniques developed by different research groups, using the methodology described in the previous section [4, 7]. In the first report (Hoover *et al.* [4]), the two best performing algorithms are the one by the University of Bern (UB) and University of Edinburgh (UE). The algorithm developed by the UB, is based on the fact that the points in any row(or column) of the range image belonging to a planar surface should be a straight line in the 3-D space. Then the idea is to divide every row(or column) of the image into sections of straight lines followed by a clustering process of lines instead of pixels. The UE algorithm is based on a region growing segmentation algorithm. It can be divided in four main steps: 1. Estimation of normal vector/Data smoothness. 2. First segmentation based on the values of curvature measures (H-K). 3. Region growing of the surface normals. 4. refinement of the calculation of borders between regions. It is worth mentioning that the last step is performed by computation the intersection between adjacent surfaces in order to achieve a more precise localization. In the second technical report by (X. Jiang *et al.* [7]), the best performance was to the the University of Osaka (UO) algorithm which is based on the analysis of the intersection of the scene with arbitrary planar surfaces.

The results of the complete segmentation process are shown in Figures 9 and 10. For the sake of clarity both Figures include the ground truth image.

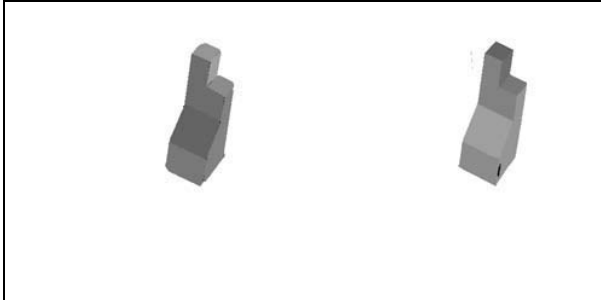


Figure 9: Segmentation result(left). Ground truth(right). (1 and 2).

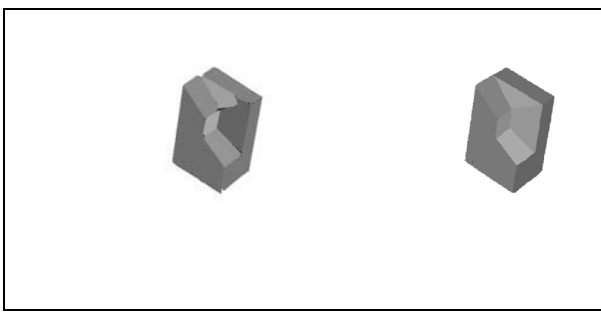


Figure 10: Segmentation result(left). Ground truth(right). (2 and 2).

The comparison methodology described in *Section 2* was used in order to determine the performance of this approach. There are some considerations that need to be taken into account in order to perform a good comparison. First, it is important to notice that for some of the segmentation techniques, special treatment was needed for the background and support planes. Furthermore, the fact that these two planes are constant for all the images introduce a strong bias in the result. This can induce a wrong interpretation of the performance indexes given that the two regions are significantly bigger than the regions under analysis and consequently are classified as "*Correct Detection*" even for a highly restrictive values of the tolerance parameter  $T$ . It is also important to notice that with this comparison methodology the interpretation of the indexes can be hard because of high variations in the size of the regions as well as in the ratio between the area and its perimeter.

In order to reduce this effect on the performance indexes some changes in the database were made. The support and background planes were removed and we only used images with one object in the scene. Figure 11 presents the percentage of *Correct Detection* for the algorithm developed at the University of Bern (UB) and for our algorithm (PB). There are three performance curves for the PB algorithm with the following interpretation: *PB with Borders*. For the performance of the segmentation technique with the parametric boundary detection presented in this paper *PB without background*. For the performance of the original segmentation technique without taking into account the support and background planes in the computation of the index *PB with background*. For the performance of our original segmentation technique developed taking into account the support and background planes in the computation of the index but not in the segmentation.

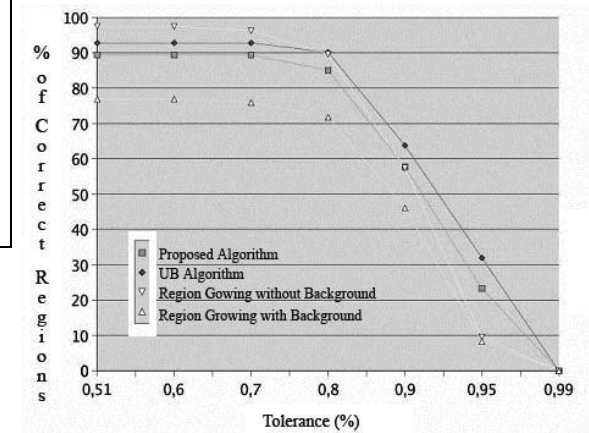


Figure 11: *Correct detection* for PB with Border, UB, PB without Background, PB with Background.

## 6 Conclusion

The parametric representation of boundaries allows a reduction in the dimensionality and the formulation is suitable to be extended to second order surfaces or a more general representation (i.e. higher order Bézier).

This technique is strongly dependant on the quality of the detected depth and orientation discontinuities. For this reason significant loss in the boundaries will lead undesirable deformations of the final representation.

According to the bibliographic review, the segmentation algorithms that use global information present higher performance with the indexes that was chosen. In this test the same tendency was found once the information provided by the parametric re-intersection of the segmented surface was included in the algorithm.

The optimality criteria used in our segmentation technique is a function of the error between the parametric model obtained in the segmentation process and the original range data. It is important to make clear that this criteria is not necessarily equivalent to the optimal performance obtained with hand made segmentation performed by experts, given that in the last result it is clear that the use of subjective criteria related to global characteristics of the surfaces was involved. This reasoning can be extrapolated to several segmentation techniques based on local properties that has been evaluated with the same comparison methodology, presenting in general a lower performance.

The performance indexes are strongly dependant on the geometric characteristics of the segmented region, by its size and shape. In future work it should be interesting to study the behavior of the performance indexes as a function of these characteristics given that some of the tests performed in this paper shows some preliminary results in this direction.

The type of images in the database used for the performance analysis produce a significant influence in the value of indexes. Particularly the repetition of objects or the repetition of surfaces like the background and the support plane. One should really reconsider the inclusion or not of these two surfaces in the analysis.

**Acknowledgements:** The authors would like to thanks the National University of Colombia and the University of Alberta for their institutional support in the development this work.

- [4] A. Hoover *et al.*, An experimental comparison of range image segmentation algorithms, IEEE Transactions on PAMI, 18(7): 673-689,1996.
- [5] A. Hoover *et al.*, A Methodology for Evaluating Range Image Segmentation Techniques, IEEE Workshop on Applications for Computer Vision (WACV), 1996.
- [6] X. Jiang, K. Bowyer, Y. Morioka, S. Hiura, K. Sato, S. Inokuchi, M. Bock, C. Guerra, R.E. Locke, J.M.H. du Buf . Further Results of Experimental Comparison of Range Image Segmentation Algorithms. In 16 International Conference on Pattern Recognition, September 2000.
- [7] X. Jiang *et al.*, Some Further Results of Experimental Comparison of Range Image Segmentation Algorithms, 16 International Conference on Pattern Recognition, 2000.
- [8] X. Jiang and H. Bunke, Fast segmentation of range images by scan line grouping, Machine Vision Application, vol. 7, no. 2, pp. 115122, 1994.
- [9] M. Kass *et al.*, Snakes: Active Contour Models, International Journal for Computer Vision, 321-331, 1988.
- [10] J. Min, M. Powell, and K. W. Bowyer, Automated Performance Evaluation of Range Image Segmentation Algorithms, IEEE Transactions on Systems, Man, and Cybernetics PART B: CYBERNETICS, VOL. 34, NO. 1, pp. 263-271, February 2004.
- [11] M. W. Powell *et al.*, Comparing curved-surface range image segmenters, Proc. of the 6th ICCV, Bobmby, India, 286-291, 1998.
- [12] University of Southtern Florida Range Image Database, <http://marathon.csee.usf.edu/range/DataBase.html>
- [13] C. Xu *et al.*, Snakes, Shapes and Gradient Vector Flow, IEEE Transactions on Image Processing, Vol. 17, 359-369, 1998.
- [14] C. Xu *et al.*, Generalized Gradient Vector Flow External Forces for Active Contours, Signal Processing, 131-139, 1998.

## References

- [1] P. Boulanger, Simultaneous Segmentation of Range and Color Images Based on Bayesian Decision Theory, Canadian Conference on Computer and Robot Vision (CRV2004), London, Ontario, Canada, pp. 58-63, May 2004.
- [2] R. C. Gonzales, R. E. Woods, Digital Image Processing, Addison-Wesley, 1992.
- [3] A. Hoover; G. Jean-Baptiste; X. Jiang; P.J. Flynn; H. Bunke; D.B. Goldgof; K. Bowyer; D.W. Eggert; A. Fitzgibbon; R.B. Fisher, An experimental comparison of range image segmentation algorithms, IEEE Transactions on PAMI, 18(7), pp. 673-689,1996.